Continental Shelf Waves: Low-Frequency Variations in Sea Level and Currents Over the Oregon Continental Shelf

DAVID L. CUTCHIN[1] AND ROBERT L. SMITH

School of Oceanography, Oregon State University, Corvallis 97331

(Manuscript received 20 March 1972, in revised form 30 June 1972)

ABSTRACT

Sea level variations and currents on the Oregon continental shelf exhibit wavelike characteristics in a frequency band from approximately 0.15 to 0.45 cycle per day (cpd). Shelf wave dispersion curves and eigenfunctions for the Oregon continental shelf profile computed using a numerical technique are compared with a low-frequency (~0.03–0.75 cpd) spectral analysis of the current, sea level, and atmospheric pressure records. In a narrow band around 0.22 cpd the current, sea level relationship is consistent with the predicted values for free barotropic continental shelf waves.

1. Introduction

Continental shelf waves, topographic Rossby waves trapped over the continental margin, have frequencies less than the local inertial frequency and wavelengths much greater than the depth. The waves progress parallel to the coast in one direction only, like classical Kelvin waves: in the Northern Hemisphere they travel with their right shoulder against the coast. A computer-assisted artist's concept of a shelf wave, with the sea surface displacement greatly exaggerated, is shown in Fig. 1.

Continental shelf waves were first explicitly discussed by Robinson (1964) in a theory of quasi-geostrophic waves resonant on a sloping shelf of finite width. Mysak (1967b) extended this to include the effects of a continental slope region, deep sea stratification, and longshore current. Buchwald and Adams (1968) obtained an analytical solution for the case of an exponentially varying shelf by neglecting horizontal divergence. Niiler and Mysak (1971) examined the effect of longshore lateral shear in western boundary currents on the propagation and stability of free barotropic shelf waves. Caldwell *et al.* (1972) verified the existence of continental shelf waves in a laboratory model.

Evidence for the existence of continental shelf waves in the ocean has been found through analysis of tide-gage records from the Australian coast (Hamon, 1966; Mysak, 1967a), the Oregon coast (Mooers and Smith, 1968), and the North Carolina coast (Mysak and Hamon, 1969). On the basis of current and sea level measurements made near the island of St. Kilda (Scotland), Cartwright (1969) noted that there the diurnal tidal slot is occupied by an almost non-divergent oscillation similar to a continental shelf wave.

In order to more closely examine this phenomena an observational experiment was designed for the Oregon continental margin. The relatively uncomplicated bathymetry and low mean flow off Oregon should ease the interpretation of data collected there. Since the theory for shelf waves predicts that prominent horizontal current fluctuations accompany rather modest sea level fluctuations, it was decided to place heavy emphasis on current measurements. Because of the strong stratification and strength of the internal tide (Mooers, 1970) in the region, we were prompted to moor the three available current meters in a single vertical array to be able to distinguish any baroclinic shelf wave modes from the barotropic.

The difficulties involved in continuously measuring the distribution of wind stress and atmospheric pressure over the continental shelf, and the large uncertainties in parameterizing the momentum transfer through the sea surface from the sparse standard meteorological data available, prevented us from investigating the forced wave problem. The analysis of the observations presented in this paper is based on free shelf wave theory.

2. The experiment

a. Field measurements

Fig. 2 shows the region of the observational experiment and the principal bathymetric features of the continental margin off Oregon.

From mid-April to mid-September, 1968, a vertical array of three current meters was maintained in about 100 m of water 7 n mi off Depoe Bay. In Fig. 2, this

[1] Present affiliation: Center for Great Lakes Studies, The University of Wisconsin-Milwaukee.

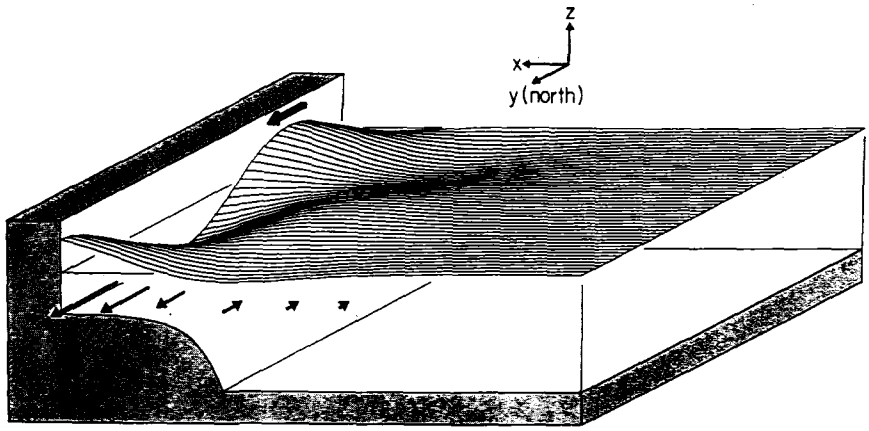

FIG. 1. A computer-assisted artist's conception of a first-mode continental shelf wave. The heavy arrow indicates direction of phase propagation and the lighter arrows indicate the water velocity under the crest. The vertical displacement of the sea surface is greatly exaggerated.

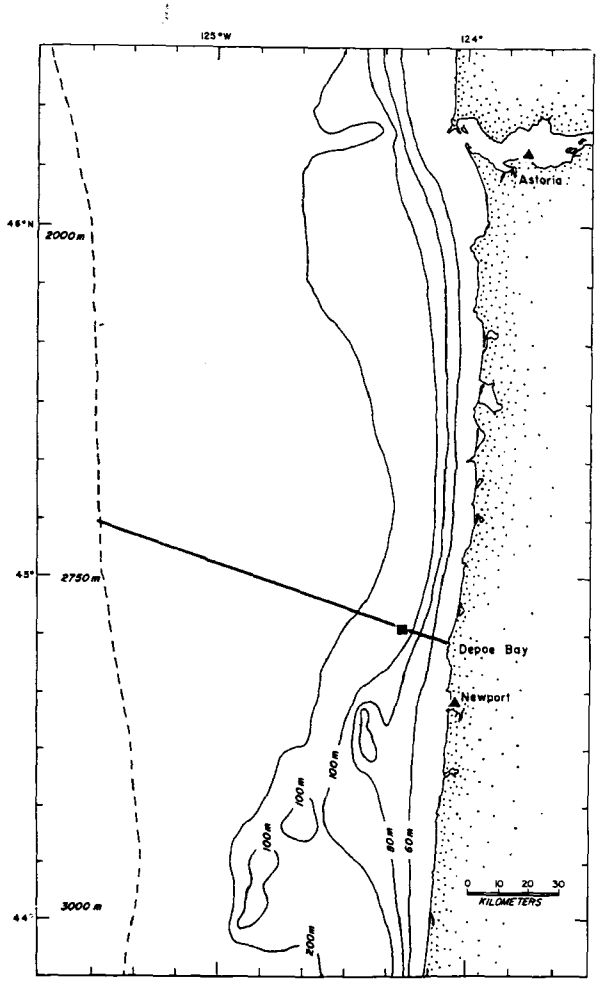

FIG. 2. The bathymetry of the experiment area. The dashed line indicates the base of the continental slope. The location of the current measurements (DB-7) is indicated by the square and the sites of the tidegages by triangles. The bathymetric profile along the line extending offshore from Depoe Bay is shown in Fig. 7.

station (DB-7) is indicated by a solid square. The current measuring devices used were Savonius rotor instruments of the Braincon-type 316. During certain periods the data sampling interval was set at 10 min and during others at 20 min. One meter was set at each of the three depths: 25, 50 and 75 m. Due to instrument failures (particularly with the instrument at 75 m) and logistic errors, a complete set of data was not obtained. The instruments were serviced and replaced at about monthly intervals. The mooring system for the meters was the taut wire array reported by Pillsbury *et al.* (1969).

Sea level elevation at the coast was provided by permanently maintained tidegages at Newport and Astoria, Ore. The tides at Newport are measured at a station 1 n mi into Yaquina Bay, a relatively small estuary without a large contributing river. The data are automatically recorded every 6 min to within 0.3 cm. Spectral tests showed very little energy in the Newport sea level record with periods <2 hr, so the data series were initially decimated to one point per hour. The tides at Astoria are measured by the National Ocean Survey (NOAA) at Tongue Point, about 12 n mi upriver from the mouth of the Columbia River estuary. The data are recorded in analog fashion and digitized every hour to within 3 cm.

Atmospheric pressure data are collected at 3-hr intervals by National Weather Service observers at Newport and Astoria.

b. The data

The digitized current meter records, in N–S and E–W component form, were passed through symmetrical low-pass filters which suppressed the diurnal tide and all higher frequencies. The filter, a "Cosine-Lanczos" taper, had a power response of 0.94, 0.5, and 0.05 at 0.42, 0.71, and 0.82 cpd, respectively. The

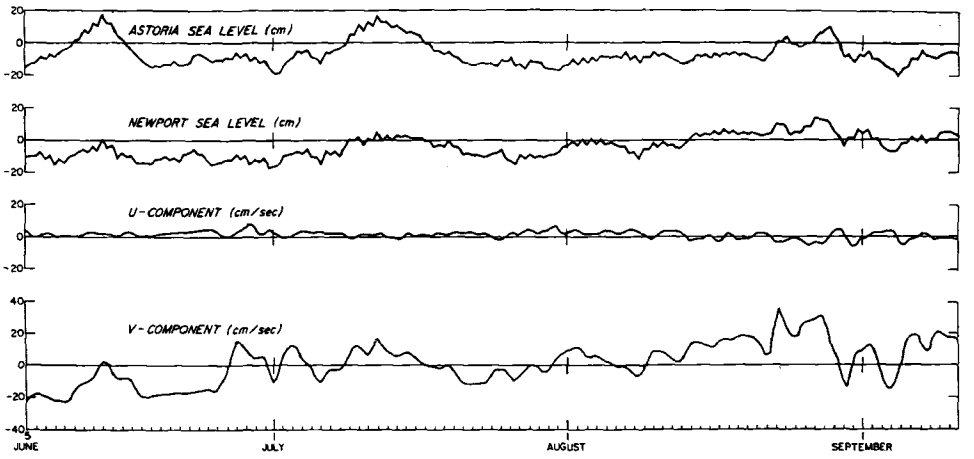

FIG. 3. Low-pass (half-power frequency is 0.71 cpd) current and sea level data.

response was below 0.01 for frequencies >0.9 cpd and between 1.0 and 1.02 for the frequency range 0.0–0.34 cpd. The records from the tidegages and the atmospheric pressure data were put through symmetrical filters with the same power response function as the filters used on the currents.

During the first 45 days of the experiment, from mid-April until the end of May, a distinct trend toward northward flow and higher sea level was readily apparent from plots of the low-passed data. A severe storm at the end of May caused substantial variations in sea level and currents as well as unusually sharp deviations from the typical late spring density structure. The statistical analysis of a single time series containing either a slow oscillation with a time scale on the order of the length of the series or an isolated burst of energy is difficult to interpret. Furthermore, the available theory for continental shelf waves goes very little beyond the treatment of small-amplitude barotropic disturbances. For these reasons we have excluded from immediate consideration the data taken during and prior to the storm. Plots of data taken during the 100 days following the storm showed activity which was, in the statistical sense, better behaved. The data record chosen for analysis extended from 0000 PST 5 June to 0000 PST 11 September, 1968.

The low-passed current records from the three depths, 25, 50 and 75 m, showed a steady shear between 25 and 75 m with the shallow water flowing more southerly than the deep water by about 10 cm sec^{-1}. The direction and magnitude of this observed shear was consistent with the slope of the isopycnals due to the seasonal coastal upwelling, i.e., the thermal wind equation appears to hold (see Collins and Pattullo, 1970). Most of the prominent low-frequency variations (frequencies <1 cpd) in the currents were uniform at all three depths; it does not appear that internal modes were greatly excited. It should be noted, however, that during the upwelling season the permanent pycnocline at DB-7, the current meter station, was located between 15 and 25 m depth. Current meters were not placed closer to the surface than 25 m in order to avoid the confusing effects of surface wind waves on the data records. Had observations been made above the pycnocline they might have shown some oscillating shears.

Because of the similarity of current fluctuations observed at the three depths, it was decided to examine in detail only the most complete of the current records. For the time frame selected for analysis, the 50 m record was the most complete with only one gap, from 1200 PST 17 June to 0000 PST 24 June, which was interpolated with a straight line.

Most of the low-frequency oscillating flows observed at DB-7 were directed along 020° true, which closely coincides with the orientation of the local depth contours. It is therefore appropriate to display the current vector components in a coordinate system with $+v$ toward 020° true and $+u$ toward 110° true (Fig. 3). The tick marks along the bottom abscissa correspond to 0000 PST on every day. The first day of each month is identified by a larger mark.

Also shown in Fig. 3 are the low-passed sea level records from Newport and Astoria. These records have been adjusted for the effect of atmospheric pressure on sea level according to the hydrostatic hypothesis, i.e., a 1-mb increase in atmospheric pressure decreases sea level by 1 cm. The high-frequency jitter on the sea level plots is due to the leakage of some of the very abundant diurnal tidal energy through the low-pass filter.

c. Autospectra

Figs. 4 and 5 show the autospectra for the data series shown in Fig. 3. A linear trend was removed from all series before analysis. The spectra have not been recolored for the effect of the low-pass filters. Over the

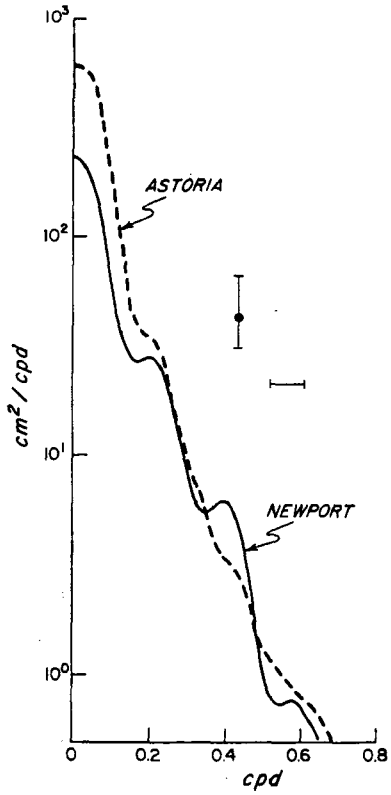

FIG. 4. Adjusted sea level spectra. The bandwidth and 80% confidence interval are indicated.

frequency range 0.0–0.8 cpd recoloring would have little effect on the shape of the curves. All of the auto-spectra show the strong peak at zero frequency and the steep roll-off characteristic of geophysical processes. Interesting, but barely significant, bumps appear at 0.22, 0.35 and 0.58 cpd.

3. Theoretical analysis

The linearized equations of motion for long waves in a shallow, homogeneous, uniformly rotating fluid are

$$\frac{\partial u}{\partial t} - fv = -g\frac{\partial \zeta}{\partial x}, \tag{1}$$

$$\frac{\partial v}{\partial t} + fu = -g\frac{\partial \zeta}{\partial y}, \tag{2}$$

where u and v are the velocity components along horizontal coordinates x and y, respectively, ζ is the elevation of the free surface above its equilibrium position, f the local Coriolis parameter, g the acceleration due to gravity, and t time. Forcing and viscous damping have been ignored. The equation of continuity is

$$\frac{\partial (hu)}{\partial x} + \frac{\partial (hv)}{\partial y} + \frac{\partial \zeta}{\partial t} = 0, \tag{3}$$

where h is the depth.

We will consider the case of a continental shelf aligned with the y axis (Fig. 1), so h varies only with x. The deep water beyond the continental shelf is assumed to be of constant depth D. We ignore the effect of the weak mean southward flow ($\sim$10 cm sec^{-1}) and the lateral shear. The Rossby number for the mean barotropic current (10^{-2}) is too small for the circulation to significantly affect the properties of the waves (Niiler and Mysak, 1971).

Following Robinson (1964) we assume wavelike solutions of angular frequency σ and wavenumber k which propagate in the y direction, i.e.,

$$(u,v,\zeta) = \{u_0(x), v_0(x), \zeta_0(x)\} \exp i(ky - \sigma t).$$

Inserting this form into (1) and (2), we obtain

$$u_0(x) = ig(-\sigma\zeta_0' + fk\zeta_0)(\sigma^2 - f^2)^{-1}, \tag{4}$$

$$v_0(x) = g(\sigma k\zeta_0 - f\zeta_0')(\sigma^2 - f^2)^{-1}, \tag{5}$$

where the primes indicate derivatives with respect to x. Substituting these expressions into (3), the equation of continuity, we can obtain one differential equation in $\zeta_0(x)$:

$$\sigma[h(\zeta_0'' - k^2\zeta_0) + h'\zeta_0'] - fh'k\zeta_0 + g^{-1}\sigma(\sigma^2 - f^2)\zeta_0 = 0. \tag{6}$$

This equation is to be solved subject to the boundary condition $hu_0 = 0$ at the shoreline ($x = 0$). Through (4)

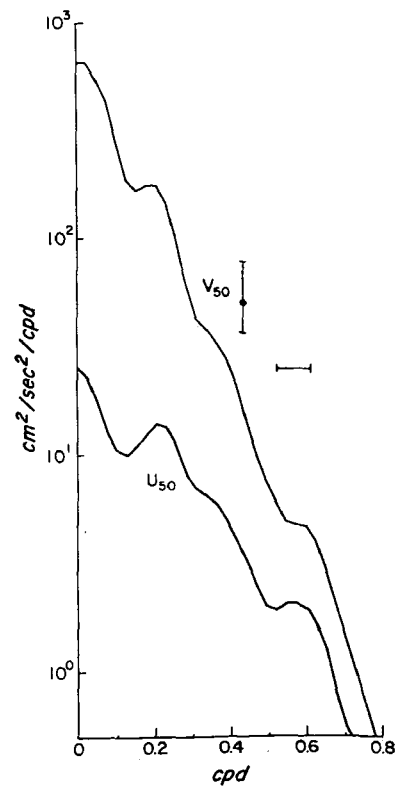

FIG. 5. Spectra for components of current in local bathymetric coordinate system ($+v$ toward 020° true).

this demands that

$$\zeta_0' = fk\sigma^{-1}\zeta_0. \tag{7}$$

Also, for a wave solution trapped against the shoreline, we require that

$$\zeta_0 \to 0 \quad \text{as} \quad x \to -\infty.$$

With h= constant, which we have assumed for the deep region beyond the foot of the slope, the solutions to (6) are in the form of increasing and decreasing exponentials. The increasing exponential form

$$\zeta_0 \propto \exp\left|g^{-1}h^{-1}(f^2-\sigma^2)+k^2\right|^{\frac{1}{2}}x \tag{8}$$

appropriately goes to zero as $x \to -\infty$.

Subject to (7) and (8), we can solve (6) by the numerical technique outlined by Caldwell and Longuet-Higgins (1972). Eq. (6) has solutions only for certain eigenvalue pairs of k and σ. The locus of these points in the k,σ plane describes the dispersion curves for the waves. Dispersion relations and eigenfunctions predicted theoretically by this method have been verified by the rotating model studies of Caldwell *et al.* (1972).

Fig. 6 shows the continental shelf wave dispersion curves computed for the depth profile off Depoe Bay. Only the first three modes and the 0th mode, the last being similar to a Kelvin wave, are shown. The slope of a line drawn between the origin and any point k,σ on the curves is proportional to $\sigma/k = C_p$, the phase speed of the wave. (Some such lines have been drawn in and their speeds indicated.) All points on the 0th mode curve have very high phase speeds quite close to the value $(gh)^{\frac{1}{2}} = 0.167$ km sec^{-1} predicted for a true Kelvin wave against a vertical wall. The dashed box in the lower left-hand corner indicates that region of the k,σ plane in which the long-wavelength, non-dispersive treatment by Robinson (1964) and Mysak (1967a) is valid.

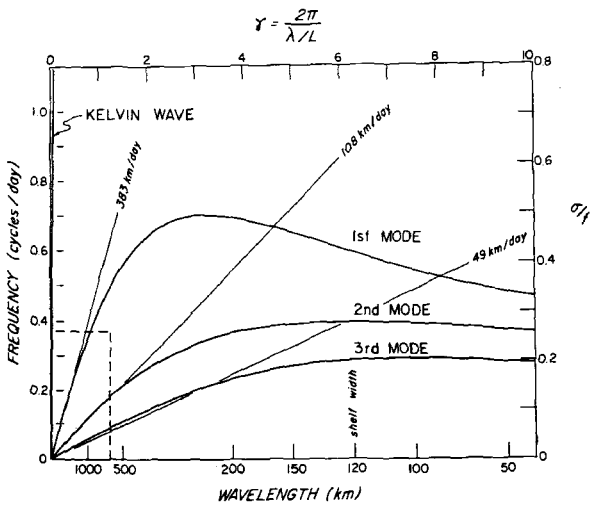

FIG. 6. Dispersion curves for the Kelvin wave mode and the first three shelf wave modes. Wavenumber is non-dimensionalized by the shelf width L.

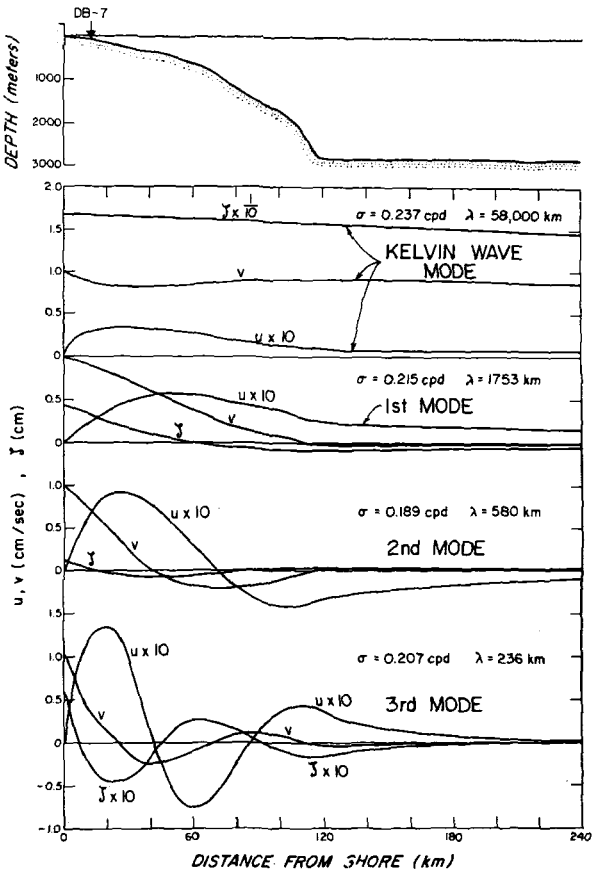

FIG. 7. Bathymetric profile extending offshore from Depoe Bay, Ore. (see Fig. 1), and selected eigenfunctions for the Kelvin wave and first three shelf wave modes.

The slope of the dispersion curve at any point k,σ is proportional to $\partial\sigma/\partial k$, the group velocity or energy transport velocity of the wave. As noted by Buchwald and Adams (1968), the direction of energy transmission for shelf waves reverses at the cutoff frequency for each mode. The direction of the phase velocity, however, remains the same (south to north along the Oregon coast).

Fig. 7 shows the eigenfunctions for the Kelvin wave mode and the first three shelf wave modes as computed by the numerical technique. The Depoe Bay shelf profile appears at the top of the figure. The particular frequency and wavelength at which each eigenfunction was separately computed appears in the figure. Note that for the equivalent Kelvin wave the onshore transport is very small, and the sea level perturbation is very large in comparison to the longshore transport. Most of the wave is transmitted along the coast in the deep sea region. For the Kelvin wave the presence of a continental shelf perturbs the eigenfunctions and the propagation characteristics to only a minor extent. The shelf waves, however, are very weak beyond the

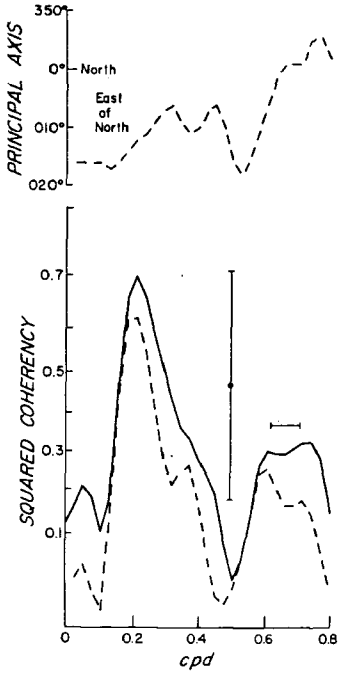

FIG. 8. Squared coherency between u and v components of the current in the local topographic system (solid line) and the principal axis system (dashed line). Orientation of principal axis system is shown. Bandwidth and 95% confidence interval are shown following Jenkins and Watts (1968). Note hyperbolic arctangent scale for squared coherency.

foot of the continental margin. The irregular squiggles visible in the eigenfunction curves are the result of irregularities in the shelf profile.

4. Examination of the data for evidence of continental shelf waves

a. Coherency and phase of current components

Eqs. (4) and (5) indicate that for shelf waves the orthogonal components of flow (u,v) should be in quadrature, i.e., out of phase by 90°. Fig. 7 shows that the current measuring station is inshore of the first node in the eigenfunction for the longshore component v. Along the Oregon Coast, where shelf waves travel from south to north, this means that the observed v should lead u, the onshore component, by 90°.

The phase relationship and coherency between the components of a vector time series depend upon the coordinate system in which the components are specified. In the theoretical consideration of shelf waves one usually assumes a straight coast of uniform cross section so the coordinate system axes are then quite naturally chosen to lie, respectively, along and perpendicular to the isobaths. However, real continental shelves are anything but straight and uniform, and the choice of the orientation of a coordinate system is not obvious. One can select any of a number of orientations for the coordinate system; e.g., the direction of the local bathymetric contours at the measurement site (020° true at DB-7), the local shelf break, or the direction of some smooth line representative of the foot of the continental shelf.

One way to resolve this quandry is to turn the problem around and specify the coordinate system orientation on a basis determined by characteristics of the data itself. A system in which the estimated phase difference between u and v is identically $\pm 90°$ is variously called the "principal axis" system, the "hodograph" system (Mooers, 1970), or the "normal axis" system (Fofonoff, 1969). The orientation of this system for the 50 m current data series is shown at the top of Fig. 8. Note that the principal axis is different for different frequencies but, in general, lies between 0° and 20° east of north. These are within the range of reasonable headings for a natural coordinate system on the Oregon Coast.

The rotation of the coordinate system into the principal axis does not fix the sign of the 90° phase shift between u and v. This is left to be determined by the data. Results of analyses of the observed currents in the principal axis system showed the predicted lag of the onshore flow (u) behind the northward longshore flow (v).

One other feature characteristic of wave motions is a strong coherency between the orthogonal components of flow because of the fixed amplitude ratio and phase

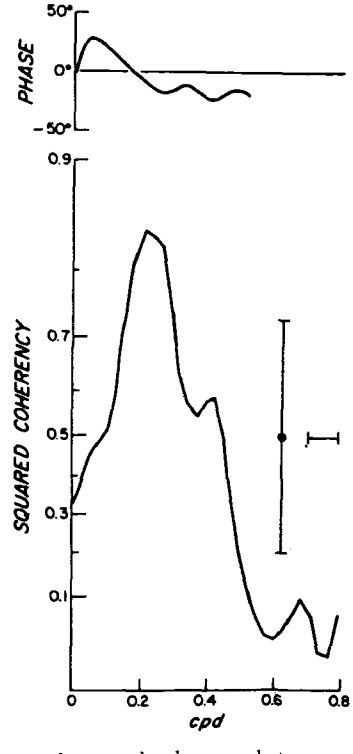

FIG. 9. Phase and squared coherency between v (in principal axis system) and Newport adjusted sea level. Phase is positive for v leading sea level and is shown only if coherency is significant.

difference [Eqs. (4) and (5)]. The solid line in Fig. 8 shows the squared coherency between u and v in the local topographic (020° true) system. There is a substantial peak at about 0.22 cpd. However, the coherency is a function of coordinate system orientation and even relatively unorganized fluid flows confined to some preferred axis, such as that of a channel or a nearby coastline, will exhibit very high u,v coherency in a system tilted at 45° to that axis. A solution to this problem is to rotate the coordinate system through all angles and determine the minimum coherence. If the minimum coherency is high, then this is strong evidence for some organizing principle such as wave motion. The dashed line at the bottom of Fig. 8 shows the minimum squared coherency observed between u and v. The coordinate system which minimizes the coherency is the same principal axis system described above. (By definition, the coherency between the components in the principal axis system is minimized.) The peak around 0.22 cpd persists and we conclude there is strong evidence for wavelike motion at about 0.22 cpd.

The autospectra of u and v in the principal axis system are not significantly different than those determined in the 020° system (Fig. 4).

b. Currents and coastal sea level

Fig. 9 shows the squared coherency and phase difference between the barometrically adjusted sea level at Newport and the v component of the current as measured in the principal axis system. The large coherency peak at about 0.22 cpd in Fig. 9 corresponds to the peak in Fig. 8. At 0.22 cpd, v measured at DB-7 lags sea level measured at Newport, by a few degrees. This is roughly consistent with the longshore separation of the stations and the predicted phase velocity of the 1st mode wave. One might expect to find a strong in-phase connection between flow to the north and the elevation of sea level at a nearby coastal station because of geostrophy. A surprising result of these observations was the banded structure of the coherency and the relatively low values at some frequencies.

c. Phase and coherency between coastal sea levels

Fig. 10 shows the squared coherency and phase between barometrically adjusted sea levels at Newport and Astoria. Again a strong peak appears at about 0.22 cpd. However, the squared coherency around zero frequency is much higher than that observed in the previous comparisons.

The phase indicates that from about 0.22 to 0.35 cpd Newport sea level leads Astoria sea level by about 40°. This phase shift between these two stations, 180 km apart, implies a total wavelength of 1620 km. Knowledge of the wavelength and frequency from the observations allows one to make a comparison with the theoretical curve (Fig. 7). Over a range of frequencies

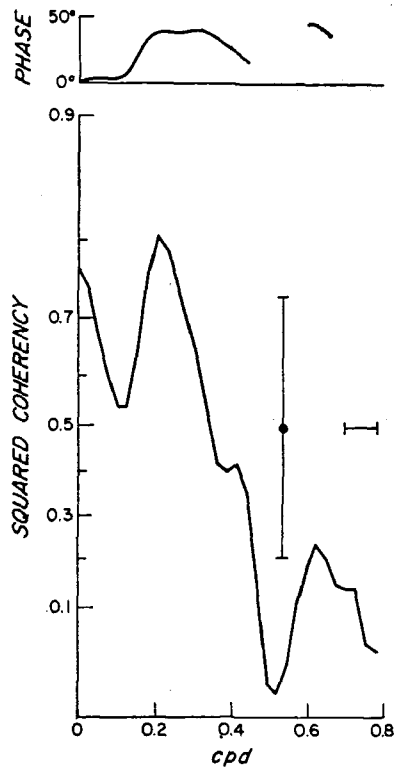

FIG. 10. Phase and squared coherency between Newport and Astoria adjusted sea level (Newport leads Astoria).

between 0 and 0.3 cpd the observed values compare closely to the dispersion curve predicted for the first mode. There is, however, some ambiguity in the interpretation of the phase information. The indicated shift between the two stations could be ± an integral multiple of 360°. If Newport sea level leads Astoria sea level by 40°+360°, this corresponds to a wavelength of 170 km. The dispersion curves in Fig. 6 show that this would be consistent with a third-mode wave at 0.22 cpd. However, tidegage data from temporary stations located between Newport and Astoria during the 1930's indicates that the phase difference increases only slowly with distance from Newport. This supports the interpretation of a phase difference of only 40° and a wavelength of 1620 km, and excludes the short wavelength (<300 km) third-mode waves.

There exists an intriguing qualitative relationship between the squared coherency spectra shown here and some features of the shelf wave dispersion curves. Note first that each of the squared coherency spectra (Figs. 8–10) have three significant peaks—one prominent peak around 0.22 cpd and two lesser peaks at about 0.4 and 0.65 cpd. Fig. 11 contains a typical squared coherency spectrum, in this case longshore current (012° coordinate system, the principal axis system for 0.22 cpd) vs sea level at Newport placed alongside the dispersion curves shown in Fig. 5. The peaks happen to coincide with the inversion points or

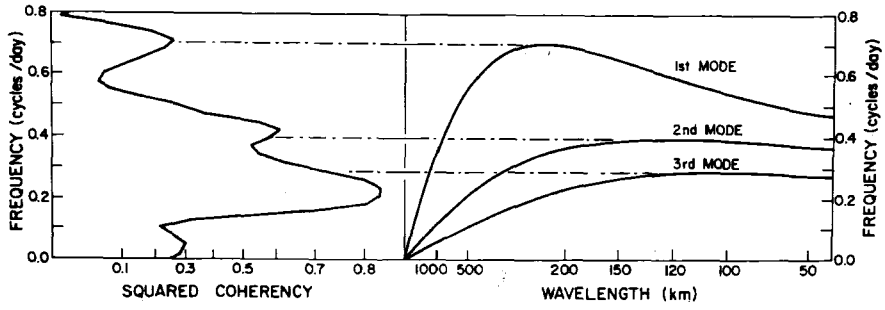

FIG. 11. Dispersion curves (from Fig. 6) compared with a typical coherency spectrum (v in 012° true coordinate system vs Newport adjusted sea level).

maxima in the dispersion curves for the first three shelf wave modes. It is tempting to believe that this is more than accidental. Indeed, Buchwald and Adams (1968) have suggested that shelf wave modes might be resonant at those lengths and frequencies where their dispersion curves leveled off and turned over. In these regions of zero group velocity the energy supposedly cannot propagate away from the generating area. Strong unimodal wave motions in certain frequency bands could peak up the coherencies among current components and sea levels. Low or multimodal wave energy in other bands could drive the coherency way down. This would explain the otherwise mysterious "line" structure in the coherency spectra. The major flaw in this interpretation is the necessity of associating the peak at 0.22 cpd with the third mode shelf wave.

Shelf wave generation theories show that wave modes are preferentially excited by wind stress and pressure disturbances which match the free wave's phase speed and wavelength. It should be possible to determine the modal composition of the shelf wave from knowledge of the characteristics of the forcing functions. The major pressure fluctuations along the coast, as determined from a series of stations 200 km or so apart, had length scales >1000 km. This, again, supports the first mode interpretation (wavelength >1000 km) for the 0.22-cpd disturbance. The only available wind data are based on geostrophic computations from the pressure field. Analysis of the sea level and current observation in terms of forced waves demands more complete and sophisticated meteorological measurements than were available.

d. Amplitude ratios for variations in currents and sea levels

Although the free wave theory used here can say nothing about the absolute magnitude of current and sea level oscillations, it does predict the magnitude of the variation in one observable relative to the variation in another. These relative values or magnitude ratios may be determined, as a function of frequency, from eigenfunctions such as those shown in Fig. 7. Table 1 contains some selected comparisons between observed and predicted ratios. All of the entries correspond to 0.22 cpd, the frequency of the prominent peak in the coherency spectra. The observed amplitude ratios are taken as simply the square root of the ratio of the power spectral estimates for the individual parameters. The values of the squared coherencies between the parameters have also been included.

The first row in Table 1 compares variations in longshore flow vs variations in onshore-offshore flow (in the principal axis system). Predicted amplitude ratios are listed for the first three modes. Observed current ratios appear to be third mode waves although there are certain complicating circumstances. For the first mode the oscillations in the longshore flow are predicted to be many times those in the onshore-offshore flow. Because of irregularities in the bathymetry it is unreasonable to expect that this extremely elongated pattern could exist undisturbed. The onshore-offshore flow might also be preferentially augmented by motions due to internal modes. Comparison between current records obtained at different depths showed considerably more vertical shear in the onshore-offshore flow than in the longshore flow.

The second row in Table 1 matches variations in longshore flow against variations in barometrically adjusted sea level as measured at Newport. Note that in this case the coherency is quite high. This may be due to freedom from contamination by internal modes such as those affecting the onshore-offshore flow. The observed amplitude ratio between sea level and longshore flow closely fits that predicted for the first mode. It should be noted that the ratio for the third mode is quite sensitive to the exact form of the predicted

TABLE 1. Ratios of velocity components and sea level at 0.22 cpd.

	Observed	Predicted $(P/P)^{\frac{1}{2}}$	Mode
U and V	$(P_{vv}/P_{uu})^{\frac{1}{2}}=3.9$	34	1
		9.9	2
	$\gamma_{uv}^2=0.63$	3.3	3
V and sea level	$(P_{ss}/P_{vv})^{\frac{1}{2}}=0.4$	0.36	1
		0.18	2
	$\gamma_{sv}^2=0.83$	0.15	3

eigenfunction since the current measurement station, DB-7, is close to a node in the eigenfunction (Fig. 7). Within the uncertainties, the magnitude of the predicted ratio could be adjusted by a factor of 2 or 3 and brought into coincidence with the observed ratio.

5. Conclusions

In a limited band of frequencies between about 0.2 and 0.3 cpd, observations made of coastal currents and sea levels are consistent with the theoretically predicted form for a first-mode free continental shelf wave. The evidence for a first mode rather than other low mode numbers is primarily on the basis of the phase lag between sea levels measured along the coast.

There remain a number of interesting clues that the third mode might also be present. The resolution of the problems regarding modal structure would require a more extensive array of sensors. In addition to more current meter stations along and across the shelf, one would be interested in one or more deep-sea tidegage records taken at points a few tens of kilometers out from the foot of the slope. Since shelf waves are almost completely confined to the shelf region they would not appear on the deep gages. Kelvin wave crests, however, extend far into the ocean basin and would cause almost the same surface elevations off the shelf as at the sea coast. With this information one could remove the Kelvin wave contributions from the observed sea levels and study the residual for shelf waves. The relatively high sea level perturbations associated with the Kelvin wave mode may have caused some of the difficulties encountered in the interpretation of these data.

The restriction of shelf wave phenomena to only certain frequency bands remains as one of the most interesting and puzzling observations made during this experiment. The autospectra of the sea levels, currents, and atmospheric pressure are relatively smooth yet the coherency spectra all exhibit strong peaks. The observed phase differences between sea level variations along the coast do not support a simple explanation based on the resonance mechanism suggested by Buchwald and Adams (1968). One possible explanation is a selectively depressed coherency due to the overlapping energy from another mode. For example, let us assume that most of the energy from 0.2–0.5 cpd is in 1st mode waves and that the high-frequency cutoff for the 3rd mode is at a frequency just below 0.2 cpd. If there is some sort of resonance associated with cutoff frequencies then the 3rd mode could contribute a substantial amount of energy just below 0.2 cpd. Depending upon the coherency between the 1st and 3rd mode, this could enhance or depress the coherency between the current vectors and the sea levels.

It has been noted (C. H. Mortimer, private communication) that the frequencies of the coherency peaks at 0.22, 0.4 and 0.65 cpd are almost in the ratio 1:2:3. Hence, the smaller peaks might be harmonics produced through nonlinear interactions. This suggests that a bispectral analysis, in the manner of Hasselmann *et al.* (1963), might profitably be applied. The theory of nonlinear Kelvin and continental shelf waves by Smith (1972) shows that the wave forms are significantly perturbed only after propagating distances equivalent to several wavelengths from the generation area. Recent studies show a striking similarity in the local wind and the current measurements over the Oregon continental shelf between 0.2 to 0.7 cpd (Huyer and Pattullo, 1972). This suggests a relatively local origin and it is unlikely that nonlinear effects have had the opportunity to develop significantly.

The remainder of the discrepancies between theory and observation are probably the result of the inability to incorporate the effects of local generation, density stratification, and irregular topography.

Acknowledgments. We are grateful for the advice and helpful critiques of Douglas Caldwell (Oregon State University) and Christopher Mooers (University of Miami) and the assistance of Dale Pillsbury, who managed the field measurements at Oregon State University. The financial support for the research was provided by the Office of Naval Research and by the National Science Foundation under Grant GA 1435.

REFERENCES

Buchwald, V. T., and J. K. Adams, 1968: The propagation of continental shelf waves. *Proc. Roy. Soc. London*, **A305**, 235–250.

Caldwell, D. R., and M. S. Longuet-Higgins, 1972: The experimental generation of double Kelvin waves. *Proc. Roy. Soc. London*, **A326**, 39–52.

——, D. L. Cutchin and M. S. Longuet-Higgins, 1972: Some model experiments on continental shelf waves. *J. Marine Res.*, **30**, 39–55.

Cartwright, D. E., 1969: Extraordinary tidal currents near St. Kilda. *Nature*, **223**, 928–932.

Collins, C. A., and J. G. Pattullo, 1970: Ocean currents above the continental shelf off Oregon as measured with a single array of current meters. *J. Marine Res.*, **28**, 51–68.

Fofonoff, N. P., 1969: Spectral characteristics of internal waves in the ocean. *Deep-Sea Res.*, **16** (Supplement), 59–72.

Hamon, B. V., 1966: Continental shelf waves and the effects of atmospheric pressure and wind stress on sea level. *J. Geophys. Res.*, **71**, 2883–2893.

Hasselmann, K., W. Munk and G. MacDonald, 1963: Biospectra of ocean waves. *Proc. Sym. Time Series Analysis*, M. Mosenblatt Ed., New York, Wiley, 125–139.

Huyer, A., and J. G. Pattullo, 1972: A comparison between wind and current observations over the continental shelf off Oregon, summer 1969. *J. Geophys. Res.*, **77**, 3215–3220.

Jenkins, G. M., and D. G. Watts, 1968: *Spectral Analysis and Its Applications.* San Francisco, Holden-Day, 525 pp.

Mooers, C. N. K., 1970: The interaction of an internal tide with the frontal zone of a coastal upwelling region. Ph.D. thesis, Oregon State University.

——, and R. L. Smith, 1968: Continental shelf waves off Oregon. *J. Geophys. Res.*, **73**, 549–557.

Mysak, L. A., 1967a: On the very low frequency spectrum of the sea level on a continental shelf. *J. Geophys. Res.*, **72**, 3043–3047.

——, 1967b: On the theory of continental shelf waves. *J. Marine Res.*, **25**, 205–227.

——, and B. V. Hamon, 1969: Low frequency sea level behavior and continental shelf waves off North Carolina. *J. Geophys. Res.*, **74**, 1397–1405.

Niiler, P. P., and L. A. Mysak, 1971: Barotrophic waves along an eastern continental shelf. *Geophys. Fluid Dyn.*, **2**, 273–288.

Pillsbury, D., R. L. Smith and R. C. Tipper, 1969: A reliable low-cost mooring system for oceanographic instrumentation. *Limnol. Oceanog.*, **14**, 307–311.

Robinson, A. R., 1964: Continental shelf waves and the response of sea level to weather systems. *J. Geophys. Res.*, **69**, 367–368.

Smith, Ronald, 1972: Non-linear Kelvin and continental shelf waves. *J. Fluid Mech.*, **52**, 379–391.